

## ORIGINAL ARTICLE

# Role of microbiota-derived corisin in coagulation activation during SARS-CoV-2 infection

Tatsuki Tsuruga<sup>1</sup> | Hajime Fujimoto<sup>1</sup> | Taro Yasuma<sup>1,2,3,4</sup> |  
 Corina N. D'Alessandro-Gabazza<sup>2,3,5</sup> | Masaaki Toda<sup>2</sup> | Toshiyuki Ito<sup>1</sup> |  
 Atsushi Tomaru<sup>1</sup> | Haruko Saiki<sup>1</sup> | Tomohito Okano<sup>1</sup> | Manal A. B. Alhawsawi<sup>5,6</sup> |  
 Atsuro Takeshita<sup>1,4</sup> | Kota Nishihama<sup>4</sup> | Reoto Takei<sup>7</sup> | Yasuhiro Kondoh<sup>7</sup> |  
 Isaac Cann<sup>5,6,8,9</sup> | Esteban C. Gabazza<sup>2,3,5</sup> | Tetsu Kobayashi<sup>1,3</sup>

<sup>1</sup>Department of Pulmonary and Critical Care Medicine, Faculty and Graduate School of Medicine, Mie University, Tsu, Mie, Japan

<sup>2</sup>Department of Immunology, Faculty and Graduate School of Medicine, Mie University, Tsu, Mie, Japan

<sup>3</sup>Microbiome Research Center, Mie University, Tsu, Mie, Japan

<sup>4</sup>Department of Diabetes, Endocrinology and Metabolism, Faculty and Graduate School of Medicine, Mie University, Tsu, Mie, Japan

<sup>5</sup>Carl R. Woese Institute for Genomic Biology, University of Illinois at Urbana-Champaign, Urbana, Illinois, USA

<sup>6</sup>Division of Nutritional Sciences, University of Illinois Urbana-Champaign, Urbana, Illinois, USA

<sup>7</sup>Department of Respiratory Medicine and Allergy, Tosei General Hospital, Seto, Aichi, Japan

<sup>8</sup>Department of Animal Science, University of Illinois Urbana-Champaign, Urbana, Illinois, USA

<sup>9</sup>Department of Microbiology, University of Illinois at Urbana-Champaign, Urbana, Illinois, USA

## Correspondence

Esteban C. Gabazza, Department of Immunology, Mie University Graduate School of Medicine, Edobashi 2-174, Tsu,

## Abstract

**Background:** Coagulopathy is a major cause of morbidity and mortality in COVID-19 patients. Hypercoagulability in COVID-19 results in deep vein thrombosis, thromboembolic complications, and diffuse intravascular coagulation. Microbiome dysbiosis influences the clinical course of COVID-19. However, the role of dysbiosis in COVID-19-associated coagulopathy is not fully understood.

**Objectives:** The present study tested the hypothesis that the microbiota-derived proapoptotic corisin is involved in the coagulation system activation during SARS-CoV-2 infection.

**Methods:** This cross-sectional study included 47 consecutive patients who consulted for symptoms of COVID-19. A mouse acute lung injury model was used to recapitulate the clinical findings. A549 alveolar epithelial, THP-1, and human umbilical vein endothelial cells were used to evaluate procoagulant and anticoagulant activity of corisin.

**Results:** COVID-19 patients showed significantly high circulating levels of corisin, thrombin-antithrombin complex, D-dimer, tumor necrosis factor- $\alpha$ , and monocyte-chemoattractant protein-1 with reduced levels of free protein S compared with healthy subjects. The levels of thrombin-antithrombin complex, D-dimer, and corisin were significantly correlated. A monoclonal anticorisin-neutralizing antibody significantly inhibited the inflammatory response and coagulation system activation in a SARS-CoV-2 spike protein-associated acute lung injury mouse model, and the levels of corisin and thrombin-antithrombin complex were significantly correlated. In an *in vitro* experiment, corisin increased the tissue factor activity and decreased the anticoagulant activity of thrombomodulin in epithelial, endothelial, and monocytic cells.

**Conclusion:** The microbiota-derived corisin is significantly increased and correlated

Manuscript handled by: Roger Preston

Final decision: Roger Preston, 13 February 2024

Tatsuki Tsuruga, Hajime Fujimoto, and Taro Yasuma contributed equally to this work.

© 2024 The Author(s). Published by Elsevier Inc. on behalf of International Society on Thrombosis and Haemostasis. This is an open access article under the CC BY license (<http://creativecommons.org/licenses/by/4.0/>).

Mie 514-8507, Japan.

Email: [gabazza@doc.medic.mie-u.ac.jp](mailto:gabazza@doc.medic.mie-u.ac.jp)

#### Funding information

This study was financially supported in part by grants from the Japan Society for the Promotion of Science (Grant numbers 23K07651 and 22K08280), the Japan Science and Technology Agency (Grant number JPMJFR2216), the 2022 Suzuken Memorial Foundation, the 2022 Yokoyama Foundation for Clinical Pharmacology, the 2022 Japan Diabetes Foundation/Novo Nordisk Pharma Ltd, the 2022 Takeda Science Foundation, and the 2023 Takeda Science Foundation. The research of I.C. was supported by the Charles and Margaret Levin Foundation.

with activation of the coagulation system during SARS-CoV-2 infection, and corisin may directly increase the procoagulant activity in epithelial, endothelial, and monocytic cells.

#### KEYWORDS

apoptosis, coagulation, corisin, COVID-19, inflammation, microbiota

## 1 | INTRODUCTION

COVID-19 is caused by the novel SARS-CoV-2 [1]. As of December 2022, more than 600 million people worldwide had been infected with the virus, and the global number of deaths due to COVID-19 was more than 6 million [1]. The increase in excess mortality, or the number of total deaths directly or indirectly caused by the COVID-19 pandemic compared with that expected under nonpandemic conditions, is even more dramatic. The World Health Organization estimated global excess mortality of approximately 14.83 million between January 2020 and December 2021 [2]. Coagulopathy is an important factor contributing to increased morbidity and mortality in patients with COVID-19. Enhanced coagulation system activation in COVID-19 patients leads to deep vein thrombosis and thromboembolic disease that may involve multiple organs, including the lungs, brain, heart, spleen, and kidneys [3–8]. Coagulation activation in COVID-19 disease has been attributed to increased activation of platelets and enhanced expression and/or activation of procoagulant factors, including tissue factor (TF), prothrombin, factor (F) V, FVIII, FXI, FXII, and FXIII [8–11]. Hypofibrinolysis, due to reduced availability of plasminogen or increased activation of plasminogen activator inhibitor-1 and thrombin-activatable fibrinolysis inhibitor, and decreased levels of anticoagulant proteins, including protein C, protein S (PS), membrane-bound thrombomodulin (TM), and endothelial protein C receptor (EPCR), have also been reported to play a role in the pathogenesis of COVID-19-associated coagulopathy [8,12–15].

The microbiota is a complex community of microorganisms, including bacteria, that inhabits the human body. It plays a vital role in human health and disease, influencing many physiological processes, such as digestion, metabolism, immunity, and inflammation [16,17]. Dysbiosis, or a disturbance in the balance and diversity of the microbiota, can contribute to the development or severity of various diseases, such as obesity, diabetes, liver diseases, cancer, and infections [16–18]. Dysbiosis of the gut and respiratory microbiota has also been linked to the severity of acute lung injury (ALI) or acute respiratory distress syndrome (ARDS), which are life-threatening forms of respiratory

failure that can be caused by COVID-19 [19,20]. For example, the population of bacteria that promotes immune response decreases while the number of opportunistic microbes increases, and this proportionally correlates with the severity of COVID-19 [21–23]. In addition, lower diversity of the gut and respiratory microbiota has been associated with more severe COVID-19 [22,24,25]. Despite strong evidence showing the role of dysbiosis in COVID-19-associated ALI/ARDS, the responsible microbial factor involved in the pathological process remains unclear. However, we recently identified a microbiota-derived proapoptotic peptide named corisin that induces acute exacerbation of pulmonary fibrosis and ALI in experimental animal models [26,27]. The levels of corisin are also dramatically elevated in the bronchoalveolar lavage fluid (BALF) and serum from patients with idiopathic pulmonary fibrosis with acute exacerbation [28]. In addition, recent studies have shown that treatment with an anticorsin monoclonal neutralizing antibody ameliorates lipopolysaccharide-induced ALI in a preventive and established disease model, suggesting that corisin is also implicated in the pathogenesis of ALI [28,29]. Based on these findings, it is possible to speculate that corisin is one factor that can worsen the clinical course of SARS-CoV-2 infection.

The present study investigated the hypothesis that corisin is involved in the activation of the coagulation system during SARS-CoV-2 infection. To test this hypothesis, we evaluated the relationship between corisin levels and coagulation markers in COVID-19 patients and animal models with SARS spike protein-induced ALI. We also investigated whether corisin can induce the expression of TF, a key initiator of coagulation, in alveolar epithelial, endothelial, and monocytic cells.

## 2 | MATERIALS, SUBJECTS, AND METHODS

### 2.1 | Patients

This is a cross-sectional study of 47 subjects who presented to our institutions with symptoms suggestive of COVID-19 between June and December 2022 (Supplementary Figure S1, Table). COVID-19 diagnosis

was confirmed by reverse transcriptase polymerase chain reaction (PCR) using nasopharyngeal or sputum samples. The Table summarizes the patients' demographics, clinical characteristics, underlying medical conditions, treatment, and routine coagulation parameters. The cohort included 39 patients with moderate COVID-19 and 8 with severe disease (Table). Blood was sampled from all patients. The serum was separated after centrifugation and stored at  $-80^{\circ}\text{C}$  until use. Serum samples collected from 8 healthy volunteers were used as controls.

## 2.2 | Experimental animals

Male WT C57BL/6J mice were provided by Nihon SLC. The mice weighed 20 to 22 g and were 8-9 weeks old. The mice were acclimated to the new environment for 2 weeks before the experiments. The mice were housed in a specific pathogen-free facility at  $21^{\circ}\text{C}$  and a 12-hour light/dark cycle in the Experimental Animal House of Mie University. In their cages, we provided the mice with wood-wool nesting material, water, and food *ad libitum*.

## 2.3 | Ethical statement

The Ethical Committee of Mie University for Clinical Investigation (approval number: U2022-012, date: May 19, 2022) approved the clinical study protocol. The clinical work followed the Helsinki Declaration. Written informed consent was obtained from all subjects. The experimental protocol for the animal model was approved by the Animal Investigation Committee of Mie University (approval number: 2021-5-SAI1, date: May 16, 2023). All experiments were conducted under the internationally approved laboratory animal care principles published by the National Institutes of Health (<https://olaw.nih.gov/>). The research also followed the Animal Research: Reporting of In Vivo Experiments (ARRIVE) Guidelines for animal investigation.

## 2.4 | ALI experimental model

Eight mice received an anticorin-neutralizing monoclonal antibody (mAb), while 9 received an isotype immunoglobulin (Ig) G control at a dose of 20 mg/kg body weight via intraperitoneal injection. The injections were administered every other day for a total of 4 doses over 1 week. On day 8, 1 day after the final antibody treatment, mice were anesthetized using inhaled isoflurane and placed in the supine position. An incision was made in the anterior neck region to expose the trachea. Mice treated with the anticorin mAb or control IgG received an intratracheal administration of a mixture comprising high molecular weight polyinosinic-polycytidylic acid (Poly-IC) (7.5 mg/kg of body weight) and recombinant SARS spike protein (0.6 mg/kg of body weight), followed by 100  $\mu\text{L}$  of air. Control mice were administered

TABLE Clinical parameters of the COVID-19 patients.

Clinical data	Normal range	Values
Age, y (mean $\pm$ SD)		77.36 $\pm$ 11.71
Sex		
Male		26
Female		21
Body mass index		20.18 $\pm$ 4.06
Smoking		
Never		20
Current smoker		24
Ex-smoker		3
Arterial pressure		
Systolic	( $\leq 120$ mm Hg)	133.28 $\pm$ 32.74
Diastolic	( $\leq 80$ mm Hg)	77.31 $\pm$ 18.68
Respiratory frequency	(12-20/min)	23.27 $\pm$ 7.22
SpO <sub>2</sub>	(95%-100%)	93.93 $\pm$ 4.63
Body temperature	(36.5-37.2 $^{\circ}\text{C}$ )	37.66 $\pm$ 1.17
General coagulation parameters		
Prothrombin time	(9-13 sec)	12.77 $\pm$ 3.21
Activated partial thromboplastin time	(24-39 sec)	37.73 $\pm$ 13.07
Fibrinogen (mg/dL)	(200-400 mg/dL)	409.57 $\pm$ 125.21
Fibrin degradation products	(<5.0 $\mu\text{g}/\text{mL}$ )	7.95 $\pm$ 10.05
Disease severity		
Moderate		39
Severe		8
Underlying diseases		
Arterial hypertension		12
Cardiopathy		9
Cerebral vascular disease		8
Interstitial lung disease		7
Cancer		6
Diabetes mellitus		5
COPD		5
Dementia		5
Rheumatoid arthritis		4
Chronic kidney disease		3
Allergy		3
Sarcoidosis		1

(Continues)

TABLE (Continued)

Clinical data	Normal range	Values
Treatment		
Anti-inflammatory drugs		22
Corticosteroids		17
Antibiotics		20
Antiviral drugs (remdesivir)		22

Data are the mean  $\pm$  SD.

COPD, chronic obstructive pulmonary disease; COVID-19, coronavirus disease 2019; SPO<sub>2</sub>, saturation of percutaneous oxygen.

intraperitoneal injections of saline following the same schedule as the antibody treatment. They then underwent intratracheal instillation of the same volume of saline or the dose of Poly-IC or recombinant SARS spike protein. All mouse groups underwent computed tomography (CT) after 24 hours, and blood, BALF, and lung samples were collected after 28 hours of intratracheal infusion under profound anesthesia.

## 2.5 | Biochemical analysis

The concentrations of cytokines, chemokines, coagulation markers, Toll-like receptor-3 (TLR3), fatty-acid binding protein-2 (FABP-2), and corisin were measured by enzyme immunoassays as described in the [Supplementary Material](#).

## 2.6 | Phosphatidyl serine externalization assay

Human umbilical vein endothelial cells (HUVECs,  $4 \times 10^5$  cells/well) were cultured in 12-well plates until sub-confluent, and after serum starvation for 12 hours, they were treated with corisin or a scrambled peptide, and phosphatidyl serine externalization was evaluated after 48 hours by flow cytometry (FACScan, BD Biosciences) after staining with fluorescein-labeled annexin V and propidium iodide (FITC-Annexin V Apoptosis Detection Kit with PI, Biolegend) [26].

## 2.7 | Immunohistochemical staining

The terminal deoxynucleotidyl transferase dUTP nick end labeling (TUNEL) assay and fibrinogen/fibrin (goat anti-mouse fibrinogen/fibrin) staining were performed at MorphoTechnology Corporation in Sapporo, Hokkaido, Japan, using standard procedures.

## 2.8 | CT examination

A Hitachi Aloka Medical micro-CT Latheta LCT-200 was used for the radiological study. Mice were anesthetized with inhaled isoflurane and

placed in a prone position as described before [30]. The ALI radiological findings were scored as described [29]. Seven experts in the field blindly scored the CT findings.

## 2.9 | BALF sampling

BALF was collected from mice under deep anesthesia prior to euthanasia, as described previously [31]. The BALF samples were centrifuged, and the supernatant was stored at  $-80^\circ\text{C}$  until analysis. The cells were counted with a nucleocounter (ChemoMetec). The BALF cells were smeared on a glass slide using a cytospin and stained with May-Grünwald Giemsa (Merck) for differential cell counting.

## 2.10 | Lung sampling

The lungs were collected after mouse euthanasia by isoflurane overdose, as described previously [32]. After thoracotomy, the pulmonary circulation was flushed with saline, and the lungs were removed. One lung was fixed in formalin, embedded in paraffin, and stained with hematoxylin-eosin. Histopathological findings were assessed using an Olympus BX50 microscope with a plan objective and an Olympus DP70 digital camera.

## 2.11 | ALI severity assessment

The ALI severity was assessed using a scoring system based on previously reported histopathological findings, including the accumulation of neutrophils, the presence of a hyaline membrane, interstitial thickening, microthrombi formation, atelectasis, and hemorrhage [29]. Each finding was scored as follows: 0 for absent, 1 for focal, and 2 for diffuse findings. The sum of the scores for each finding was taken as the total score.

## 2.12 | Cell culture

A549 and THP-1 cells were maintained in RPMI 1640 medium (Nacalai Tesque), while HUVECs were cultured in EGM-2 (Lonza Japan) medium. Both cell lines were incubated at  $37^\circ\text{C}$  in a humidified atmosphere containing 95% air and 5% CO<sub>2</sub>. Each culture medium was supplemented with 10% (v/v) heat-inactivated fetal bovine serum, 100 IU/mL penicillin, and 100  $\mu\text{g}/\text{mL}$  streptomycin.

## 2.13 | TF activity

HUVEC, THP-1, and A549 cells were cultured in a 48-well plate until subconfluent. After overnight starvation, 5  $\mu\text{M}$  corisin, scrambled peptide, or 12.5  $\mu\text{g}/\text{mL}$  Poly-IC with or without anticorisin mAb was added and

incubated for 24 hours. The cells were washed with 4-2-hydroxyethyl-1-piperazineethanesulfonic acid (HEPES)-buffered saline and then 200  $\mu$ L of a mixture containing 10 nM FVIIa and 200 nM FX in HEPES-buffered saline with 5 mM  $\text{CaCl}_2$  and 1 mM  $\text{MgCl}_2$  was added along with 10  $\mu$ g/mL of anti-TF antibody. Following incubation for 30 minutes at 37 °C, 90  $\mu$ L of the reaction mixture was removed and added to 10  $\mu$ L of phosphate-buffered saline containing 100 mM EDTA to stop FXa formation. The reaction mixture was transferred to a 96-well plate, and 10  $\mu$ L of S-2222 (final concentration 0.2 mM) was added and incubated for 30 minutes at room temperature. The reaction was stopped with 10  $\mu$ L of 30% acetic acid, and the absorbance at 405 nm was measured.

## 2.14 | TM activity

HUVEC, THP-1, and A549 cells were seeded in a 48-well plate until subconfluent. After overnight starvation, 5  $\mu$ M corisin, scrambled peptide, or 12.5  $\mu$ g/mL Poly-IC with or without anticorisin mAb was added and incubated for 24 hours. The cells were then washed with HEPES-buffered saline (10 mM HEPES, 150 mM NaCl, 4 mM KCl, 11 mM glucose, pH 7.5), and 200  $\mu$ L of a mixture containing 80 nM protein C and 0.05 U/mL thrombin in HEPES-buffered saline with 5 mM  $\text{CaCl}_2$ , and 1 mM  $\text{MgCl}_2$  was added along with anti-TM antibody (clone R7D7). The reaction was incubated for 60 minutes at 37 °C. After incubation, 90  $\mu$ L of the reaction mixture was removed and added to 10  $\mu$ L of hirudin (2 U/mL). The reaction mixture was then transferred to a 96-well plate, and 10  $\mu$ L of S-2366 (final concentration 0.2 mM) was added and incubated for 30 minutes at room temperature. The reaction was stopped with 10  $\mu$ L of 30% acetic acid, and the absorbance at 405 nm was measured.

## 2.15 | Gene expression analysis

Total RNA was extracted from HUVEC lysates using Trizol Reagent (Invitrogen). The oligo-dT primers and the Superscript Preamplification System Kit (Invitrogen) were used to reverse-transcribe RNA, and then DNA was amplified by PCR. Primers' sequences are described in [Supplementary Table S1](#). The PCR conditions were as follows: 26 to 35 cycles depending on the gene, denaturation at 94 °C for 30 seconds, annealing at 65 °C for 30 seconds, and elongation at 72 °C for 1 minute, followed by a further extension at 72 °C for 5 minutes. We normalized gene expression by the GAPDH transcription level.

## 2.16 | Statistical analysis

Data are expressed as the mean  $\pm$  SD. Differences between 2 variables were calculated by Student's *t*-test and between 3 or more variables by 1-way analysis of variance (ANOVA) with the Newman-Keuls test. Variables with skewed distribution were evaluated by

the Mann-Whitney U-test or the Kruskal-Wallis ANOVA with Dunn's test. Correlations were evaluated by Pearson product-moment correlation or Spearman's correlations. Statistical analyses were done using Graphpad Prism version 9.0 (Graphpad Software). Statistical significance was considered as  $P < .05$ .

## 3 | RESULTS

### 3.1 | Increased circulating corisin and inflammatory cytokines in COVID-19

Serum levels of corisin and the inflammatory markers tumor necrosis factor- $\alpha$  (TNF $\alpha$ ) and monocyte-chemoattractant protein-1 (MCP-1) were significantly increased in COVID-19 patients compared with healthy subjects ([Figure 1A](#)). Furthermore, a significant correlation was observed in the serum levels of corisin and MCP-1 ( $r = 0.3$ ;  $P = .03$ ) across all subjects. These findings imply that corisin is released from the microbiome as part of the inflammatory response to SARS-CoV-2 infection.

### 3.2 | Coagulation system activation in COVID-19

Circulating levels of the coagulation activation markers TF, D-dimer, and thrombin-antithrombin (TAT) complex were significantly elevated in COVID-19 patients compared with healthy subjects. In addition, the free PS levels were significantly reduced in patients with COVID-19 compared with healthy subjects. Serum TM levels were increased, while serum total PS levels were reduced in COVID-19 patients compared with controls, although the differences were not statistically significant. These observations indicate that activation of the coagulation system in COVID-19 is associated with decreased activity of anticoagulant proteins ([Figure 1B, C](#)).

### 3.3 | Correlation between corisin and coagulation markers

Serum levels of corisin were positively and significantly correlated with serum levels of TAT and D-dimer, while they were negatively and significantly correlated with serum levels of total and free PS ([Figure 2](#)). These findings suggest the possibility that corisin may play a role in the activation of the coagulation system in COVID-19 patients.

### 3.4 | Sex exerts no effect on any parameter

Male and female patients with COVID-19 exhibited no significant differences in any of the measured parameters ([Supplementary Table S2](#)).

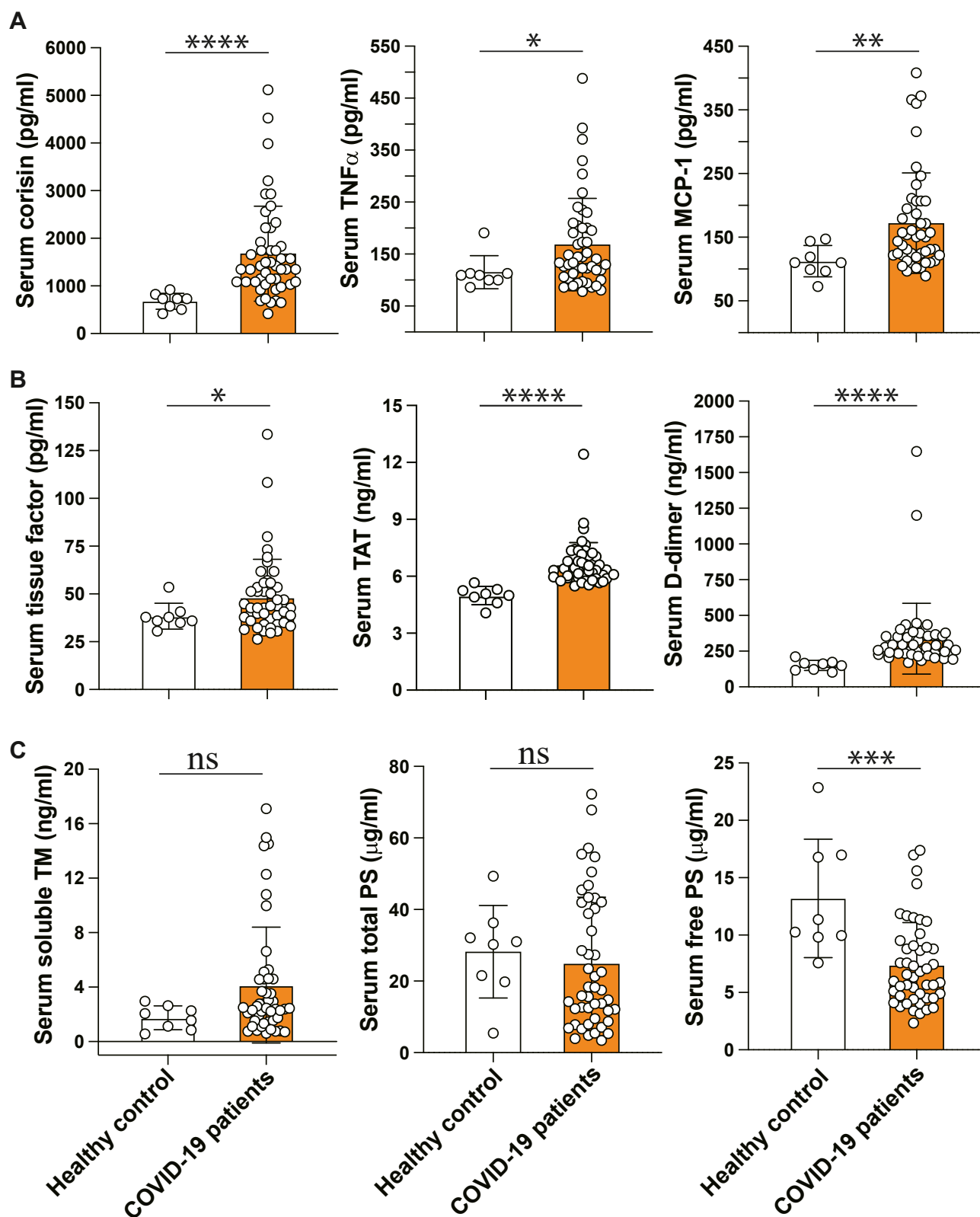


FIGURE 1 Increased serum levels of corisin, inflammatory cytokines, and coagulation activation markers in COVID-19. Corisin, tumor necrosis factor- $\alpha$  (TNF $\alpha$ ), monocyte-chemoattractant protein-1 (MCP-1), tissue factor, thrombin antithrombin (TAT), D-dimer, soluble thrombomodulin (TM), total protein S (PS), and free PS were measured by enzyme immunoassays. Data are expressed as mean  $\pm$  SD. Statistical analysis was performed by ANOVA with the Newman-Keuls test. \* $P < .05$ ; \*\* $P < .01$ ; \*\*\* $P < .001$ ; \*\*\*\* $P < .0001$ . Ns, not significant.

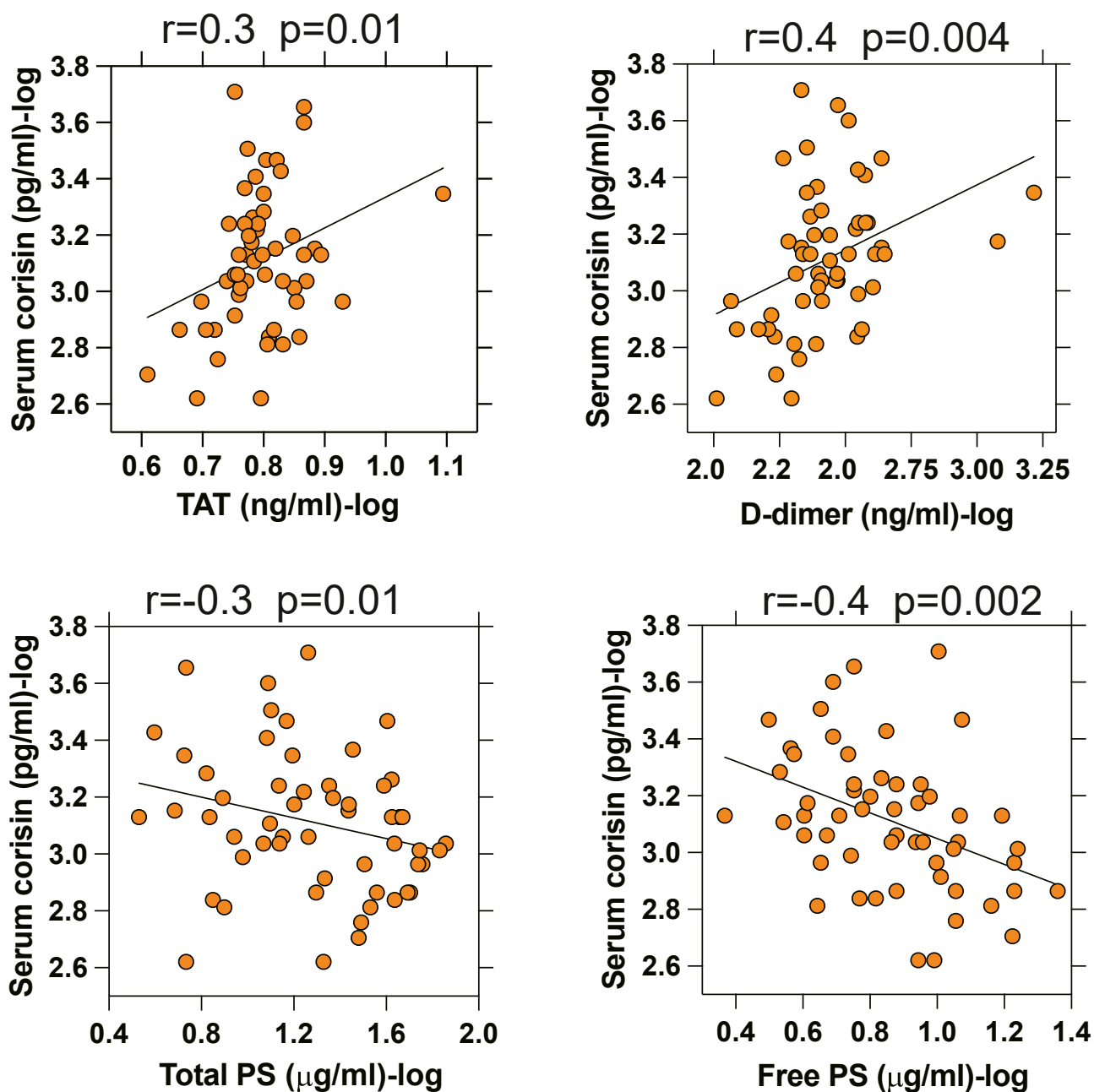


FIGURE 2 Correlation between corisin and coagulation markers in COVID-19. The relationship between corisin and coagulation markers in COVID-19 was evaluated using Pearson product-moment correlation after logarithmization of corisin, thrombin-antithrombin complex (TAT), D-dimer, total protein S (PS), and free PS due to skewed distribution. A  $P < .05$  was considered significant.

### 3.5 | Corisin plays a role in SARS spike protein-associated ALI

To clarify the involvement of the microbiota-derived corisin in the pathogenesis of SARS-CoV-2 infection, we evaluated whether an anticorisin mAb exerts any effect in a SARS spike protein-associated ALI (Supplementary Figure S2). Intratracheal instillation of a combination of Poly-IC + SARS spike protein significantly induced ALI-associated radiological (eg, ground glass opacity) and histopathological (eg, inflammatory cell infiltration and alveolar wall thickening) abnormalities

compared with the control groups. Bleeding was not observed in any mouse group. However, pretreatment with anticorisin mAb significantly improved the radiological and histopathological findings compared with pretreatment with an irrelevant antibody (Figure 3A-D).

Mice with ALI showed a significant increase in the number of inflammatory cells and a significant elevation in the levels of MCP-1, interleukin (IL)-1 $\beta$ , and IL-6 in BALF compared with mouse counterparts treated with an irrelevant antibody (Figure 4A-C). In addition, the lung tissue areas with TUNEL-positive staining were significantly increased in mice with ALI treated with IgG compared with control mice.

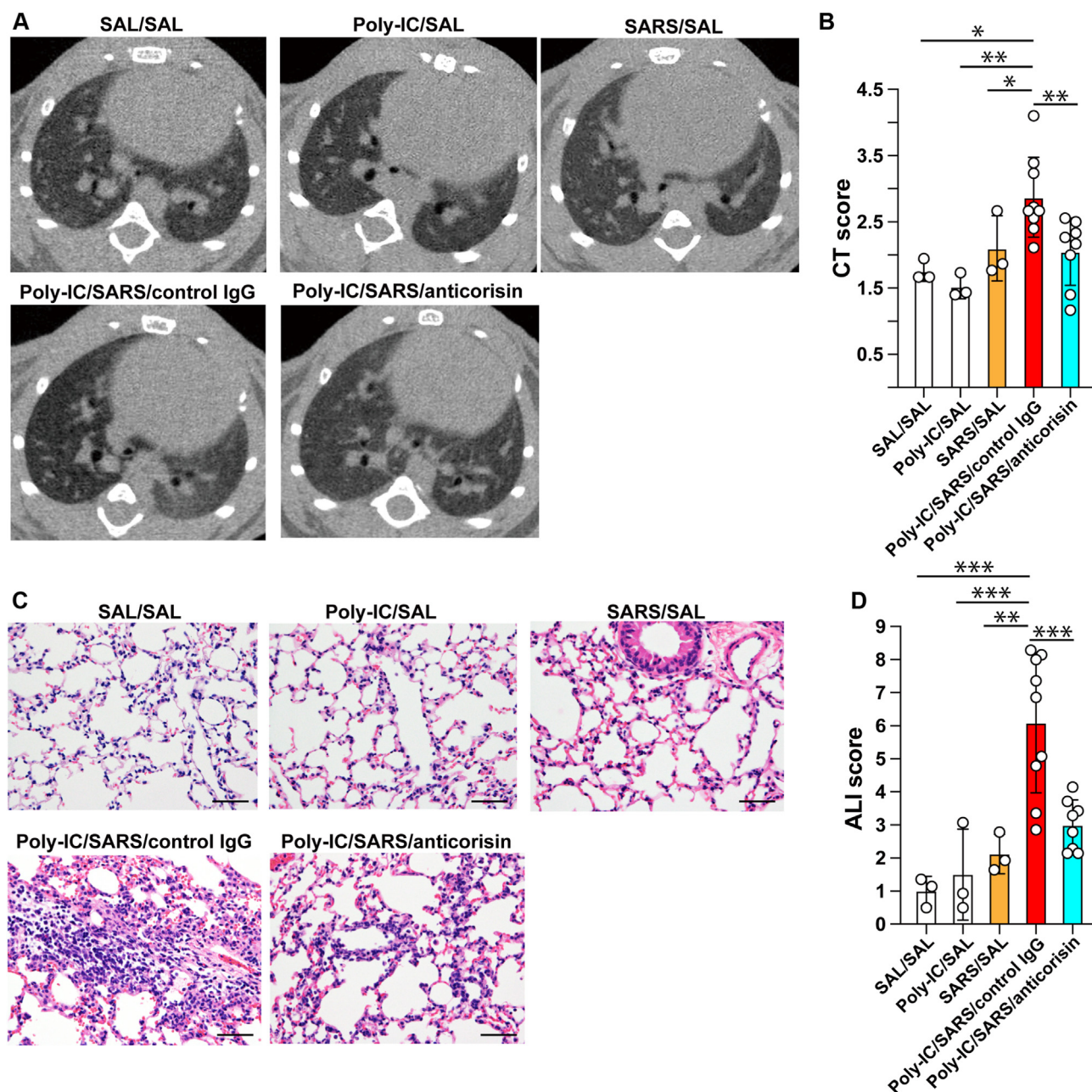


**FIGURE 3** Anticorisin antibody improves radiological and histopathological findings in mice with acute lung injury (ALI). Mice were pretreated with anticorisin monoclonal antibody (anticorisin) or irrelevant immunoglobulin (Ig) G (control IgG) 4 times by intraperitoneal injection before receiving 1 dose of intratracheal instillation of high molecular weight polyinosinic-polycytidylic acid (Poly-IC) in combination with recombinant SARS spike protein (SARS). Control mice were pretreated with physiological saline (SAL) by intraperitoneal injection 4 times before receiving intratracheal instillation of SAL, Poly-IC, or SARS. Findings of computed tomography (CT) (A, B) and hematoxylin eosin-stained lung tissue (C, D) were scored as described in the Materials and Methods section. Number of mice:  $n = 3$  in each SAL/SAL, Poly-IC/SAL, and SARS/SAL group,  $n = 9$  in the Poly-IC/SARS/IgG group, and  $n = 8$  in the Poly-IC/SARS/anticorisin group. Data are expressed as the mean  $\pm$  SD. Statistical analysis was performed using ANOVA with the Newman-Keuls test. \* $P < .05$ ; \*\* $P < .01$ ; \*\*\* $P < .001$ .

However, mice with ALI treated with anticorisin mAb had significantly decreased TUNEL-positive staining compared with counterpart mice treated with control IgG (Figure 4D, E).

These observations recapitulate the implication of the microbiota-derived corisin in the pathogenesis of SARS-CoV-2 infection.

### 3.6 | Corisin inhibition ameliorates coagulation abnormalities

Mice with ALI treated with an irrelevant antibody had significantly higher levels of fibrinogen, TF, and TAT in the BALF and lung tissue



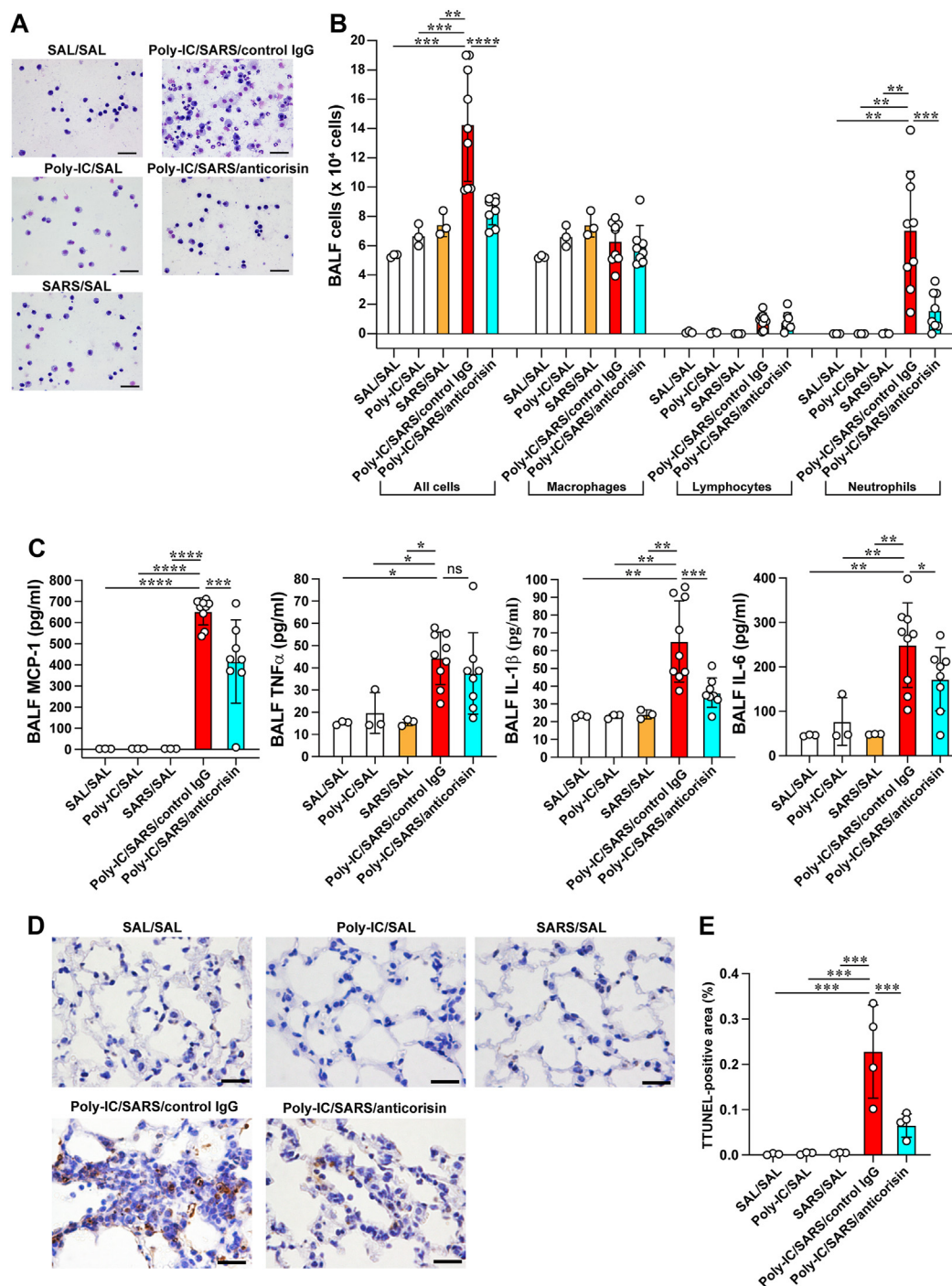


**FIGURE 4** Anticorin antibody reduces inflammatory cell infiltration, cytokine release, and apoptosis in mice with acute lung injury. Bronchoalveolar lavage fluid (BALF) was collected, and cells were counted using a nucleocounter. Differential cell counts were performed after Giemsa staining (A, B). Scale bar 20  $\mu$ m. Monocyte-chemoattractant protein-1 (MCP-1), tumor necrosis factor- $\alpha$  (TNF $\alpha$ ), interleukin (IL)-1 $\beta$ , and IL-6 were measured using commercial enzyme immunoassay kits. Number of mice in B and C:  $n = 3$  in the physiological saline (SAL)/SAL, high molecular weight polyinosinic-polycytidylic acid (Poly-IC)/SAL, and recombinant SARS spike protein (SARS)/SAL groups;  $n = 9$  in the Poly-IC/SARS/control immunoglobulin (Ig) G group; and  $n = 8$  in the Poly-IC/SARS/anticorin group. The terminal deoxynucleotidyl transferase dUTP nick end labeling (TUNEL) assay was performed as described in the Materials and Methods section, and the stained area was quantified. Histological examination of the lungs was performed using an Olympus BX50 microscope with a plan objective and an Olympus DP70 digital camera. To quantify the TUNEL-positive stained area, an investigator blinded to the treatment group randomly took microphotographs of 5 microscopic fields from each mouse lung and measured the TUNEL-positive area using the WinRoof image processing software (Mitani Corp) (D, E). Scale bar 50  $\mu$ m. Number of mice in D and E:  $n = 3$  in the SAL/SAL, Poly-IC/SAL, and SARS/SAL groups, and  $n = 4$  in the Poly-IC/SARS/IgG and Poly-IC/SARS/anticorin groups. Data are expressed as the mean  $\pm$  SD. Statistical analysis was performed using one-way ANOVA with the Newman-Keuls test. \* $P < .05$ ; \*\* $P < .01$ ; \*\*\* $P < .001$ ; \*\*\*\* $P < .0001$ . Ns, not significant.

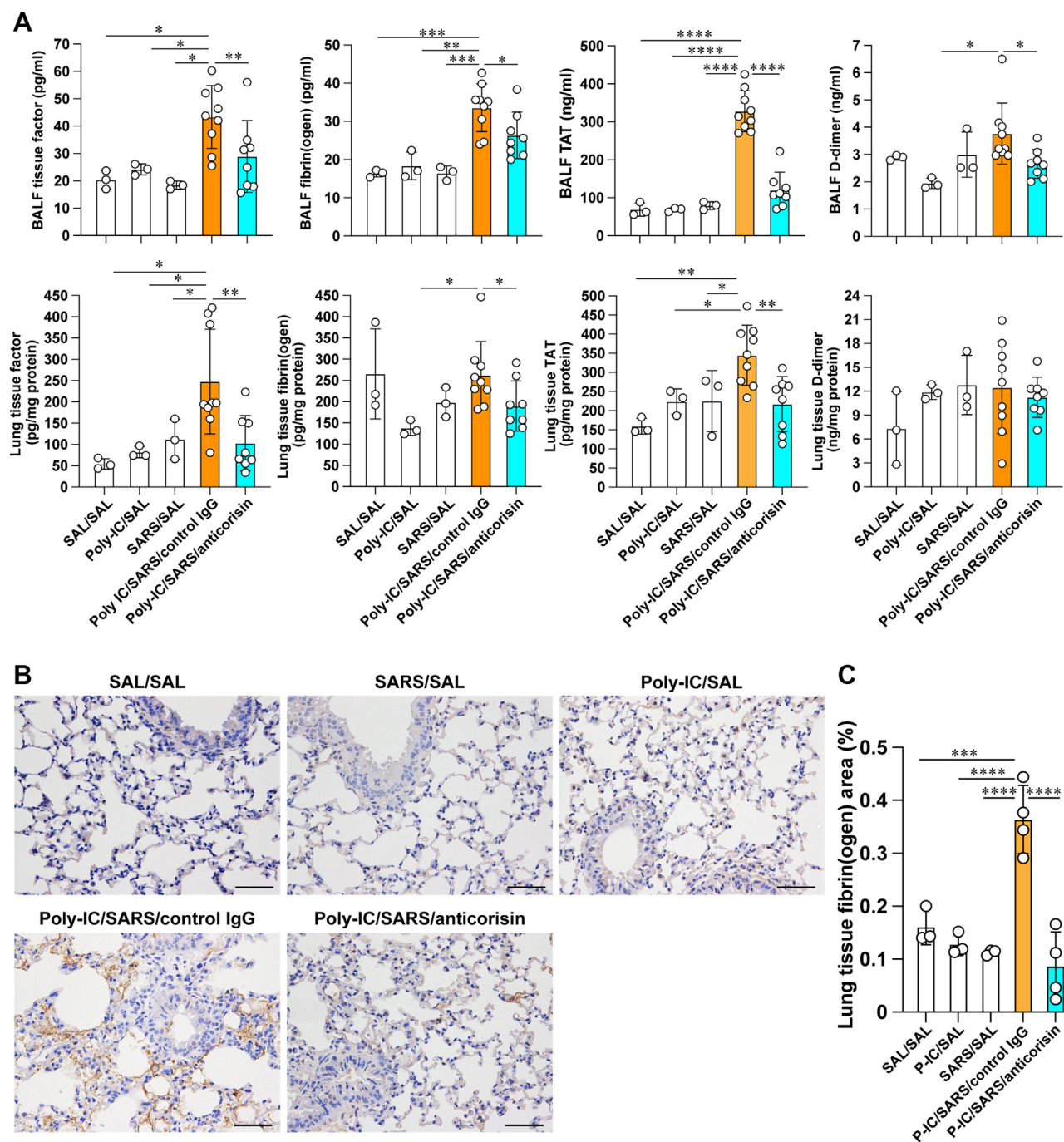


**FIGURE 5** Anticorisin antibody reduces markers of coagulation activation in mice with acute lung injury. Bronchoalveolar lavage fluid (BALF) and lung tissue were collected, and the levels of tissue factor, fibrinogen, thrombin-antithrombin complex (TAT), and D-dimer were measured by enzyme immunoassays (A). Lung tissue was stained for fibrinogen/fibrin, and the stained area was quantified. Histological examination of the lungs was performed using an Olympus BX50 microscope with a plan objective and an Olympus DP70 digital camera. To quantify the fibrinogen/fibrin-positive stained area, an investigator blinded to the treatment group randomly took microphotographs of 5 microscopic fields from the lung of each mouse and measured the fibrinogen/fibrin stained area using the WinRoof image processing software (Mitani Corp) (B, C). Scale bar 50  $\mu\text{m}$ . The number of mice in A:  $n = 3$  in the physiological saline (SAL)/SAL, high molecular weight polyinosinic-polycytidylic acid (Poly-IC)/SAL, and recombinant SARS spike protein (SARS)/SAL groups,  $n = 9$  in the Poly-IC/SARS/immunoglobulin (Ig) G group, and  $n = 8$  in the Poly-IC/SARS/anticorisin group. Number of mice in B and C:  $n = 3$  in the SAL/SAL, Poly-IC/SAL, and SARS/SAL groups, and  $n = 4$  in the Poly-IC/SARS/IgG and Poly-IC/SARS/anticorisin groups. Data are expressed as the mean  $\pm$  SD. Statistical analysis was performed using one-way ANOVA with the Newman-Keuls test. \* $P < .05$ ; \*\* $P < .01$ ; \*\*\* $P < .001$ ; \*\*\*\* $P < .0001$ .

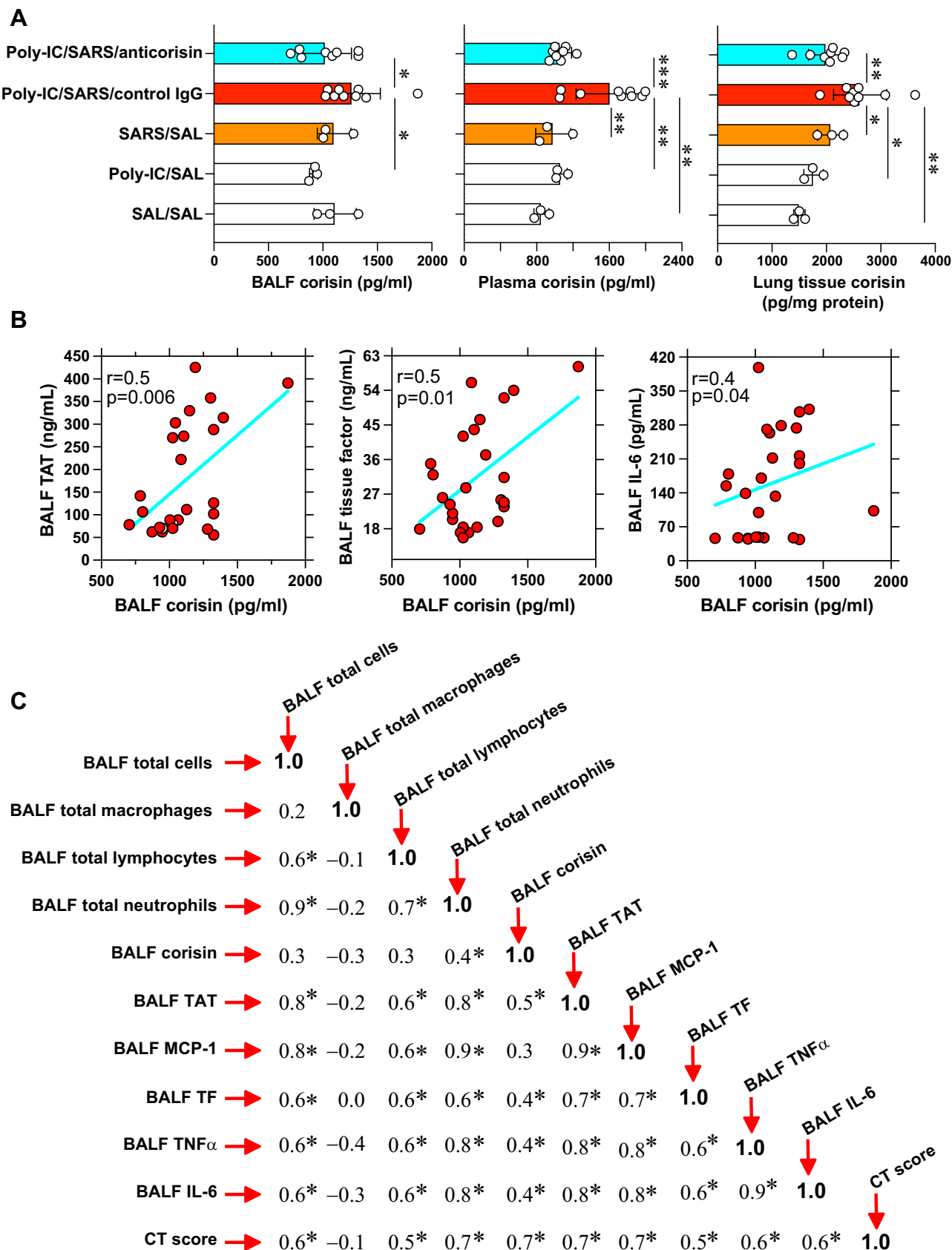


FIGURE 6 Elevated levels of corisin are correlated with SARS spike protein (SARS)-associated coagulation activation and inflammation. Corisin, markers of coagulation activation, and inflammatory cytokines were measured by enzyme immunoassays, and the relationship between the variables in bronchoalveolar lavage fluid (BALF) was evaluated by Spearman's correlation (A-C). The number of mice in each group:  $n = 3$  in

than control mice. However, mice with ALI that received the anticorin mAb had significantly lower levels of TF, fibrinogen, and TAT in the BALF and lung tissue than mice treated with control IgG. The level of D-dimer in the BALF, but not in the lung tissue, was significantly higher in mice with ALI receiving an irrelevant antibody than a control mouse or mice with ALI treated with the anticorin mAb (Figure 5A). It is worth noting that the BALF level of TAT was higher than the values previously reported, probably due to the use of different commercial immunoassay kits [33,34]. Immunohistochemical analysis demonstrated a significantly larger area of fibrinogen/fibrin staining in the lungs of ALI mice compared with control mice. Pretreatment with the anticorin mAb significantly reduced the fibrinogen/fibrin staining area compared with pretreatment with an irrelevant antibody (Figure 5B, C).

### 3.7 | Elevated corisin levels correlate with coagulation and inflammation markers

BALF, plasma, and lung tissue corisin levels were significantly higher in mice with ALI compared with control mice. Pretreatment with the anticorin mAb significantly reduced corisin levels in BALF, plasma, and lung tissue of ALI mice compared with mice treated with an irrelevant IgG (Figure 6A). In BALF, TAT and TF exhibited positive and significant correlations with corisin. Additionally, corisin levels significantly correlated with BALF neutrophil counts, inflammatory cytokine levels (TNF $\alpha$  and IL-6), and the ALI CT score (Figure 6B, C). These findings further support the role of corisin in SARS-CoV-2 infection-induced coagulation cascade activation and inflammatory response.

### 3.8 | Corisin and TLR3 level

Activation of TLR3-associated intracellular signaling is linked to an increased expression of TF and activation of the coagulation system [35]. Mice with ALI induced by Poly-IC/SARS spike protein showed significantly higher TLR3 levels than control mice. Mice with ALI treated with the anticorin mAb demonstrated lower TLR3 levels in lung tissue compared with mice treated with an irrelevant antibody, although the difference was not statistically significant. (Supplementary Figure S3). The percentage of TLR3<sup>high</sup> expression significantly increased in HUVECs and THP-1 cells stimulated with corisin compared with cells stimulated with the scrambled peptide. The corisin induction of TLR3 was significantly suppressed by the anticorin mAb in both cells. Cells cultured in the presence of Poly-IC also exhibited a significant increase in TLR3 expression, but this expression was not abrogated by the anticorin mAb (Supplementary Figure S4A-D).

### 3.9 | Gut barrier dysfunction and corisin elevation

Corisin is produced and released by commensal bacteria residing in the lungs, gut, and other organs [26]. Therefore, elevated circulating corisin levels observed in COVID-19 patients with ALI and mice with ALI might be partially attributed to gut barrier dysfunction. FABP-2, which binds and transports long-chain fatty acids in the small intestine, serves as a biomarker of intestinal barrier integrity [36]. Serum FABP-2 levels were significantly increased in COVID-19 patients compared with healthy controls. Similarly, mice with ALI exhibited significantly elevated serum FABP-2 levels compared with control mice. However, mice with ALI treated with the anticorin mAb showed significantly reduced circulating corisin levels compared with their counterparts treated with an irrelevant antibody. Further, the circulating levels of FABP-2 and corisin were significantly correlated in both COVID-19 patients and mice with ALI (Supplementary Figure S5A-D). These findings suggest that impaired gut barrier function might contribute to the increased circulating corisin levels observed in COVID-19 patients and mice with SARS spike protein-induced ALI.

### 3.10 | Corisin increases TF activity

Lung epithelial and monocytic cells are the source of TF in SARS-CoV-2 infection [9,37-39]. The role of endothelial cells as a source of TF during SARS-CoV-2 infection remains controversial [39,40]. In the present study, we stimulated HUVEC, A549, and THP-1 cells with corisin or scrambled peptide. Corisin stimulation significantly increased TF activity compared with saline control and scrambled peptide in all cells (Figure 7A). Corisin-induced TF activity was significantly inhibited in all cells pretreated with anticorin or anti-TF antibody. Poly-IC also significantly induced TF activity, but this was not affected by the anticorin mAb. This finding suggests that corisin can directly activate the coagulation system by enhancing TF activity in monocytes, alveolar epithelial cells, and endothelial cells.

### 3.11 | Corisin upregulates TF expression

HUVECs and THP-1 cells were cultured in the presence of corisin, scrambled peptide, or Poly-IC for 48 hours, and TF expression was analyzed by flow cytometry. The percentage of cells expressing high levels of TF was significantly increased by corisin or Poly-IC compared with the scrambled peptide control (Supplementary Figure S6A-D). Pretreatment of the cells with the anticorin mAb significantly suppressed TF expression induced by corisin but not that induced by Poly-IC.

the physiological saline (SAL)/SAL, high molecular weight polyinosinic-polycytidylic acid (Poly-IC)/SAL, and SARS/SAL groups,  $n = 9$  in the Poly-IC/SARS/control immunoglobulin (Ig) G group, and  $n = 8$  in the Poly-IC/SARS/anticorin monoclonal antibody (anticorin) group. Data are expressed as the mean  $\pm$  SD. Statistical analysis was performed using one-way ANOVA with the Newman-Keuls test. \* $P < .05$ ; \*\* $P < .01$ ; \*\*\* $P < .001$ . CT, computed tomography; IL, interleukin; MCP-1, monocyte-chemoattractant protein-1; TAT, thrombin-antithrombin complex; TF, tissue factor; TNF $\alpha$ , tumor necrosis factor- $\alpha$ .

This finding suggests that corisin can also promote coagulation activation by enhancing TF expression in monocytes and endothelial cells.

### 3.12 | Corisin promotes phosphatidyl serine externalization

Phosphatidyl serine is a negatively charged phospholipid normally confined to the inner leaflet of the plasma membrane [41]. Phosphatidylserine externalization facilitates coagulation activation by providing a platform for the assembly and activation of coagulation factors [41]. We have previously demonstrated that corisin induces PS externalization in alveolar epithelial cells [26,27]. Here, corisin significantly increased phosphatidyl serine externalization compared with scrambled peptide in HUVECs (Supplementary Figure S7A, B). Anticorisin mAb significantly blocked phosphatidyl serine externalization induced by corisin. Poly-IC also significantly promoted phosphatidyl serine externalization, but this effect was not suppressed by anticorisin mAb. These findings suggest that corisin may promote coagulation activation by enhancing cell phosphatidyl serine externalization, potentially contributing to its prothrombotic effects.

### 3.13 | Corisin decreases the expression and activity of TM

HUVEC, A549, and THP-1 cells were stimulated with corisin or scrambled peptide for 48 hours. After cell washing, zymogen protein C and thrombin were added, and activated protein C (APC) was measured as an indicator of TM activity [42,43]. Corisin stimulation caused a significant decrease in APC levels compared with saline and scrambled peptide in A549, THP-1, and HUVEC cells. Pretreatment with anticorisin mAb significantly reversed this effect, leading to a significant increase in APC levels compared with corisin alone in all cells (Figure 7B). Pretreatment with anti-TM antibody significantly reduced APC levels compared with cells treated with corisin alone. Poly-IC significantly reduced APC levels in all cells, but this effect was not affected by the anticorisin mAb. In addition, corisin stimulation significantly reduced the messenger RNA expression of TM and EPCRs in HUVECs (Supplementary Figure S8). These findings suggest that corisin may also promote coagulation activation by reducing the activity of TM in monocytes, alveolar epithelial cells, and endothelial cells and by downregulating the expression of TM and EPCRs in endothelial cells.

## 4 | DISCUSSION

The results of the present study show that microbiota-derived corisin is significantly released and correlated with activation of the coagulation system in COVID-19 patients and in a SARS spike protein-associated ALI mouse model and that corisin may directly increase the procoagulant activity in vascular endothelial cells, monocytes, and alveolar epithelial cells.

COVID-19 is a complex disease that affects multiple organs and systems, including the respiratory, cardiovascular, immune, and coagulation systems. The principal cause of death in COVID-19 patients is respiratory failure due to ALI and ARDS. Several studies have reported that COVID-19 patients exhibit hypercoagulability, which is associated with increased mortality and morbidity. Hypercoagulability in COVID-19 patients is manifested by elevated levels of D-dimer and other coagulation markers and increased incidence of thrombotic events, including pulmonary embolism, deep vein thrombosis, and disseminated intravascular coagulation. The mechanisms underlying the coagulation activation in COVID-19 are not fully understood. An imbalance between procoagulant factors and anticoagulant proteins due to cell injury, inflammatory cytokines, hypoxia, and direct viral infection of host cells has been suggested as possible mechanisms. Consistent with this procoagulant/anticoagulant imbalance mechanism, here we found that COVID-19 patients have increased coagulation activation associated with increased circulating levels of soluble TM and decreased circulating levels of the anticoagulant-free PS. Microbiota dysbiosis is a common feature of COVID-19 that may also contribute to coagulation activation. However, the role of dysbiosis in COVID-19-associated coagulopathy has been poorly explored. This study investigated the level of the microbiota-derived corisin and its correlation with coagulation markers in COVID-19. Corisin has been shown to induce acute exacerbation in idiopathic pulmonary fibrosis and ALI in animal models. In the present study, we found that an excessive level of corisin is positively and significantly correlated with markers of coagulation activation in COVID-19 patients. These clinical findings implicate the excessive release of the microbiota-derived corisin in the pathogenesis of COVID-19-associated coagulopathy.

The remarkable increase in the circulating level of corisin in COVID-19 is a novel finding. The result was recapitulated in the mouse ALI model induced by a mixture of SARS-CoV-2 spike protein and Poly-IC. The ALI mouse model showed markedly high level of corisin compared with control mice. Recent research reporting lung dysbiosis, with enrichment of the opportunistic and corisin-producing *Staphylococcus cohnii*, in patients who succumbed to severe COVID-19 infection further supports the pathogenic role of excessive corisin release in this disease [44]. Corisin is a 19-amino acid peptide released from a bacterial transglycosylase after degradation of the polypeptide by a bacterial protease [26]. It was originally isolated from the lung microbiome. However, whether the lung microbiome is the primary source of corisin during SARS-CoV-2 infection remains unclear. Prior investigations indicate that transglycosylases containing corisin may be secreted by various commensal or opportunistic bacteria normally found in the gut, oral, lung, or skin microbiota [26]. The association of SARS-CoV-2 infection with dysbiosis in respiratory, oral, skin, and gut microbiota [45] suggests that the microbial population from diverse body sites may contribute to the elevated corisin levels in the systemic circulation of our COVID-19 patients and mouse ALI model. This observation gains support from the high circulating and lung levels of corisin observed in patients with idiopathic pulmonary fibrosis, another well-recognized pathological condition characterized by lung, gut, and oral dysbiosis [26,28]. In our current investigation, the increased corisin level in the

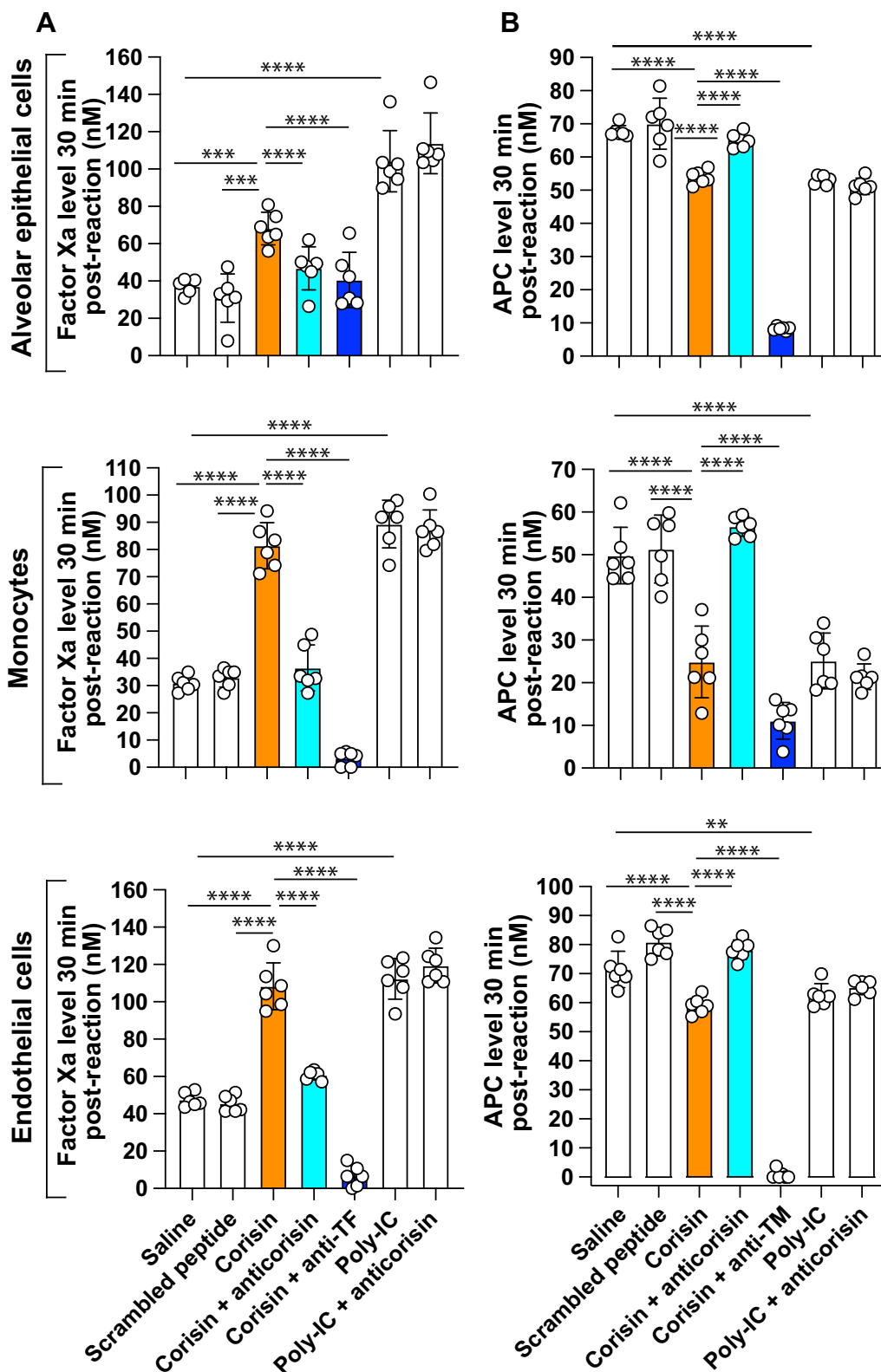


**FIGURE 7** Corisin increases tissue factor (TF) activity and decreases thrombomodulin (TM) activity. A549 alveolar epithelial cells, THP-1 cells, and human umbilical vein endothelial cells were cultured in the presence of physiological saline, corisin, scrambled peptide, or high molecular weight polyinosinic-polycytidylic acid (Poly-IC), and the activity of TF and TM was measured as described in the Materials and Methods section. Some of the cell groups were pretreated with anticorin monoclonal antibody (anticorin), anti-TF, or anti-TM antibody. Data are expressed as the mean  $\pm$  SD. Statistical analysis was performed using one-way ANOVA with the Newman-Keuls test. APC, activated protein C. \*\* $P < .01$ ; \*\*\* $P < .001$ ; \*\*\*\* $P < .0001$ .

lungs of mice with ALI points to the lung microbiota as the primary corisin source. Nonetheless, the significant correlation between the increased circulating levels of FABP-2, a marker of gut barrier injury, and corisin in both COVID-19 patients and mice with ALI suggests that the gut microbiota may serve as an additional source of corisin [36]. Furthermore, the detection of substantial corisin levels in the bile and blood of patients with severe acute cholangitis further reinforces the assumption that the alimentary tract microbiota may also potentially contribute to corisin secretion [46]. The mechanism of how dysbiosis leads to enhanced corisin release during SARS-CoV-2 infection is unclear. Notably, corisin levels are detected in both healthy subjects and normal mice, suggesting that the microbiome releases a baseline peptide level under physiological conditions [26,28]. SARS-CoV-2 infection has been documented to cause an abnormal host cell response, leading to a "cytokine storm" in conditions such as ALI or ARDS [47]. Consequently, it is conceivable that tissue injury and dysregulated host immune responses induce an overactive response in microbiome-associated organisms harboring and secreting corisin, thereby contributing to its elevated systemic release.

To clarify the role of corisin in coagulation activation associated with COVID-19, we evaluated the inhibitory activity of the anticorisin-neutralizing mAb in a mouse ALI model and different cell lines. Administration of the anticorisin mAb significantly reduces the lung levels of corisin and coagulation markers, and the radiological and histopathological signs of inflammation in ALI model. This suggests that corisin is involved in the pathogenesis of SARS spike protein-associated ALI and that blocking corisin may have a beneficial effect. Subsequently, we evaluated the relationship between coagulation system activation and corisin levels in the ALI model. There was a positive and significant correlation between corisin levels and the markers of coagulation activation TAT and TF in the mouse model. This mirrors the findings in COVID-19 patients further indicating that corisin may contribute to the coagulopathy observed in this disease. Building upon this observation, we hypothesized that corisin might directly induce procoagulant activity in cells. Our data revealed that corisin upregulates TF activity, disrupts TM-mediated anticoagulation in endothelial, alveolar epithelial, and monocytic cell lines, and enhances TF expression in endothelial and monocytic cells. Furthermore, corisin downregulates TM and EPCR expression and promotes phosphatidyl externalization and apoptosis in vascular endothelial cells. These findings are consistent with the increased expression of coagulation factors and dysfunction of the anticoagulant system reported in SARS-CoV-2 infection [48–50]. Therefore, our study suggests that corisin may directly modulate the expression and activity of procoagulant and anticoagulant proteins, leading to coagulation activation during SARS-CoV-2 infection.

In this study, we also assessed the intricate relationship between dysbiosis and inflammation by investigating the levels of corisin and inflammatory mediators in both COVID-19 patients and a mouse model of ALI. Dysbiosis has been linked to aberrant immune responses and an upregulation of inflammatory mediators. For instance, gut dysbiosis is associated with reduced production of beneficial short-chain fatty acids and an elevation in circulating cytokines [51]. Moreover, dysbiosis can release tryptophan metabolites that disrupt

the host immune response [51]. Notably, disease severity in COVID-19 patients has been associated with dysbiosis and excessive secretion of inflammatory cytokines [52]. Considering corisin's capacity to stimulate the production of inflammatory cytokines and chemokines [28], we hypothesized that an enrichment of microbiota with corisin-producing bacteria might lead to increased corisin release, triggering the secretion of inflammatory mediators from alveolar epithelial cells. Our investigation revealed a significant association between elevated circulating corisin levels and MCP-1 in COVID-19 patients. Similarly, lung corisin levels correlated with the inflammatory cytokines IL-6 and TNF $\alpha$  in the ALI mouse model. The well-established role of inflammatory cytokines in procoagulant activity during SARS-CoV-2 infection [48,49] suggests that corisin may also indirectly promote coagulation activation in COVID-19 by stimulating cytokine secretion. Conversely, corisin's procoagulant activity with enhanced thrombin generation may also contribute to increased secretion of cytokines through thrombin from other cells, including endothelial and monocytic cells [50]. This mechanism has the potential to establish a vicious cycle where corisin-mediated coagulation activation and subsequent thrombin generation drive additional cytokine secretion, further intensifying coagulation activation and thrombin generation, perpetuating inflammation, and potentially amplifying tissue damage. The inhibition of cytokines and coagulation markers by the anticorisin mAb in our ALI model provides additional support for the potential dual effect of corisin on inflammation and coagulation. In summary, therapeutically targeting corisin may not only inhibit the expression of inflammatory cytokines but also suppress the activation of the blood coagulation system. This suggests a promising avenue for alleviating the inflammatory response during SARS-CoV-2 infection.

The small sample size and descriptive design are limitations of the study in COVID-19 patients. The use of serum instead of plasma to measure coagulation parameters is another limitation in the COVID-19 study, as serum is generated after coagulation activation in non-anticoagulated blood. A limitation of the *in vitro* study is the lack of mechanistic pathways explaining how corisin promotes cell TF activity, and a limitation of the mouse ALI study is the inclusion of only male mice.

In brief, this study demonstrated that the microbiota-derived proapoptotic peptide corisin plays a crucial and direct role in the activation of the coagulation system and the inflammatory response during SARS-CoV-2 infection. However, these results need to be validated in a larger cohort of patients.

## ACKNOWLEDGMENTS

The authors are indebted and very thankful to Drs Hidenao Okuyama and Hisako Okuyama for their cooperation with this work.

## AUTHOR CONTRIBUTIONS

T.T., H.F., and T.Y. contributed equally to performing most of the experiments and preparing the first draft of the manuscript. C.N.D.'A.-G. prepared the mouse model. M.T. performed the *in vitro* study and measured several variables in the experimental animal model and clinical samples. H.S., T.I., A.T., and T.O. analyzed the clinical data. A.T.,

K.N., and M.A.B.A. analyzed the data from the experimental animal model. R.T. and Y.K. provided the clinical samples. I.C., E.C.G., and T.K. contributed to the conceptualization and design of the study, as well as the editing and correction of the manuscript. All authors have read and agreed to the final version of the manuscript.

#### DECLARATION OF COMPETING INTERESTS

E.C.G., C.N.D.'A.-G., and I.C. hold patents on corisin and the anticorisin monoclonal antibody reported in this study. The other authors declare no competing interests related to this manuscript.

#### REFERENCES

- [1] WHO. WHO Coronavirus disease (COVID-19) pandemic 2022. <https://www.who.int/publications/m/item/monthly-operational-update-on-health-emergencies-december-2022>. [accessed November 11, 2023].
- [2] Msemburi W, Karlinsky A, Knutson V, Aleshin-Guendel S, Chatterji S, Wakefield J. The WHO estimates of excess mortality associated with the COVID-19 pandemic. *Nature*. 2023;613:130–7.
- [3] Allegra A, Innao V, Allegra AG, Musolino C. Coagulopathy and thromboembolic events in patients with SARS-CoV-2 infection: pathogenesis and management strategies. *Ann Hematol*. 2020;99:1953–65.
- [4] Chan NC, Weitz JI. COVID-19 coagulopathy, thrombosis, and bleeding. *Blood*. 2020;136:381–3.
- [5] Fox SE, Akmatbekov A, Harbert JL, Li G, Quincy Brown J, Vander Heide RS. Pulmonary and cardiac pathology in African American patients with COVID-19: an autopsy series from New Orleans. *Lancet Respir Med*. 2020;8:681–6.
- [6] Jimenez D, Garcia-Sanchez A, Rali P, Muriel A, Bikdeli B, Ruiz-Artacho P, Le Mao R, Rodriguez C, Hunt BJ, Monreal M. Incidence of VTE and bleeding among hospitalized patients with coronavirus disease 2019: a systematic review and meta-analysis. *Chest*. 2021;159:1182–96.
- [7] Nannoni S, de Groot R, Bell S, Markus HS. Stroke in COVID-19: a systematic review and meta-analysis. *Int J Stroke*. 2021;16:137–49.
- [8] Sayyadi M, Hassani S, Shams M, Dorgalaleh A. Status of major hemostatic components in the setting of COVID-19: the effect on endothelium, platelets, coagulation factors, fibrinolytic system, and complement. *Ann Hematol*. 2023;102:1307–22.
- [9] Hottz ED, Azevedo-Quintanilha IG, Palhinha L, Teixeira L, Barreto EA, Pao CRR, Righy C, Franco S, Souza TML, Kurtz P, Bozza FA, Bozza PT. Platelet activation and platelet-monocyte aggregate formation trigger tissue factor expression in patients with severe COVID-19. *Blood*. 2020;136:1330–41.
- [10] McGonagle D, O'Donnell JS, Sharif K, Emery P, Bridgwood C. Immune mechanisms of pulmonary intravascular coagulopathy in COVID-19 pneumonia. *Lancet Rheumatol*. 2020;2:e437–45.
- [11] Panigada M, Bottino N, Tagliabue P, Grasselli G, Novembrino C, Chantarangkul V, Pesenti A, Peyvandi F, Tripodi A. Hypercoagulability of COVID-19 patients in intensive care unit: a report of thromboelastography findings and other parameters of hemostasis. *J Thromb Haemost*. 2020;18:1738–42.
- [12] Calderon-Lopez MT, Garcia-Leon N, Gomez-Arevalo S, Martin-Serrano P, Matilla-Garcia A. Coronavirus disease 2019 and coagulopathy: other prothrombotic coagulation factors. *Blood Coagul Fibrinolysis*. 2021;32:44–9.
- [13] Juneja GK, Castelo M, Yeh CH, Cerroni SE, Hansen BE, Chessum JE, Abraham J, Cani E, Dwivedi DJ, Fraser DD, Slessarev M, Martin C, McGilvray S, Gross PL, Liaw PC, Weitz JI, Kim PY, investigators C-B. Biomarkers of coagulation, endothelial function, and fibrinolysis in critically ill patients with COVID-19: a single-center prospective longitudinal study. *J Thromb Haemost*. 2021;19:1546–57.
- [14] Nougier C, Benoit R, Simon M, Desmurs-Clavel H, Marcotte G, Argaud L, David JS, Bonnet A, Negrier C, Dargaud Y. Hypofibrinolytic state and high thrombin generation may play a major role in SARS-COV2 associated thrombosis. *J Thromb Haemost*. 2020;18:2215–9.
- [15] Won T, Wood MK, Hughes DM, Talor MV, Ma Z, Schneider J, Skinner JT, Asady B, Goerlich E, Halushka MK, Hays AG, Kim DH, Parikh CR, Rosenberg AZ, Coppens I, Johns RA, Gilotra NA, Hooper JE, Pekosz A, Cihakova D. Endothelial thrombomodulin downregulation caused by hypoxia contributes to severe infiltration and coagulopathy in COVID-19 patient lungs. *EBioMedicine*. 2022;75:103812.
- [16] Natalini JG, Singh S, Segal LN. The dynamic lung microbiome in health and disease. *Nat Rev Microbiol*. 2023;21:222–35.
- [17] Zhang F, Aschenbrenner D, Yoo JY, Zuo T. The gut microbiome in health, disease, and clinical applications in association with the gut bacterial microbiome assembly. *Lancet Microbe*. 2022;3:e969–83.
- [18] Gilbert JA, Quinn RA, Debelius J, Xu ZZ, Morton J, Garg N, Jansson JK, Dorrestein PC, Knight R. Microbiome-wide association studies link dynamic microbial consortia to disease. *Nature*. 2016;535:94–103.
- [19] Battaglini D, Robba C, Fedele A, Tranca S, Sukkar SG, Di Pilato V, Bassetti M, Giacobbe DR, Vena A, Patroniti N, Ball L, Brunetti I, Torres Marti A, Rocco PRM, Pelosi P. The role of dysbiosis in critically ill patients with COVID-19 and acute respiratory distress syndrome. *Front Med (Lausanne)*. 2021;8:671714.
- [20] Kitsios GD, Morowitz MJ, Dickson RP, Huffnagle GB, McVerry BJ, Morris A. Dysbiosis in the intensive care unit: microbiome science coming to the bedside. *J Crit Care*. 2017;38:84–91.
- [21] Kolhe R, Sahajpal NS, Vyavahare S, Dhanani AS, Adusumilli S, Ananth S, Mondal AK, Patterson GT, Kumar S, Rojani AM, Isaacs CM, Fulzele S. Alteration in nasopharyngeal microbiota profile in aged patients with COVID-19. *Diagnostics (Basel)*. 2021;11:1622.
- [22] Zhu T, Jin J, Chen M, Chen Y. The impact of infection with COVID-19 on the respiratory microbiome: a narrative review. *Virulence*. 2022;13:1076–87.
- [23] Zuo T, Zhang F, Lui GCY, Yeoh YK, Li AYL, Zhan H, Wan Y, Chung ACK, Cheung CP, Chen N, Lai CKC, Chen Z, Tso EYK, Fung KSC, Chan V, Ling L, Joynt G, Hui DSC, Chan FKL, Chan PKS, et al. Alterations in gut microbiota of patients with COVID-19 during time of hospitalization. *Gastroenterology*. 2020;159:944, 55.e8.
- [24] Merenstein C, Liang G, Whiteside SA, Cobian-Guemes AG, Merlino MS, Taylor LJ, Glascock A, Bittinger K, Tanes C, Graham-Wooten J, Khatib LA, Fitzgerald AS, Reddy S, Baxter AE, Giles JR, Oldridge DA, Meyer NJ, Wherry EJ, McGinniss JE, Bushman FD, et al. Signatures of COVID-19 severity and immune response in the respiratory tract microbiome. *mBio*. 2021;12:e0177721.
- [25] Moreira-Rosario A, Marques C, Pinheiro H, Araujo JR, Ribeiro P, Rocha R, Mota I, Pestana D, Ribeiro R, Pereira A, de Sousa MJ, Pereira-Leal J, de Sousa J, Morais J, Teixeira D, Rocha JC, Silvestre M, Principe N, Gatta N, Amado J, et al. Gut microbiota diversity and C-reactive protein are predictors of disease severity in COVID-19 patients. *Front Microbiol*. 2021;12:705020.
- [26] D'Alessandro-Gabazza CN, Kobayashi T, Yasuma T, Toda M, Kim H, Fujimoto H, Hataji O, Takeshita A, Nishihama K, Okano T, Okano Y, Nishii Y, Tomaru A, Fujiwara K, D'Alessandro VF, Abdel-Hamid AM, Ren Y, Pereira GV, Wright CL, Hernandez A, et al. A *Staphylococcus* pro-apoptotic peptide induces acute exacerbation of pulmonary fibrosis. *Nat Commun*. 2020;11:1539.
- [27] Saiki H, Okano Y, Yasuma T, Toda M, Takeshita A, Abdel-Hamid AM, Fridman D'Alessandro V, Tsuruga T, D'Alessandro-Gabazza CN, Katayama K, Sugimoto M, Fujimoto H, Yamanaka K, Kobayashi T,



- Cann I, Gabazza EC. A microbiome-derived peptide induces apoptosis of cells from different tissues. *Cells*. 2021;10:2885.
- [28] D'Alessandro-Gabazza CN, Yasuma T, Kobayashi T, Toda M, Abdel-Hamid AM, Fujimoto H, Hataji O, Nakahara H, Takeshita A, Nishihama K, Okano T, Saiki H, Okano Y, Tomaru A, Fridman D'Alessandro V, Shiraiishi M, Mizoguchi A, Ono R, Ohtsuka J, Fukumura M, et al. Inhibition of lung microbiota-derived proapoptotic peptides ameliorates acute exacerbation of pulmonary fibrosis. *Nat Commun*. 2022;13:1558.
- [29] Fridman D'Alessandro V, D'Alessandro-Gabazza CN, Yasuma T, Toda M, Takeshita A, Tomaru A, Tharavecharak S, Lasisi IO, Hess RY, Nishihama K, Fujimoto H, Kobayashi T, Cann I, Gabazza EC. Inhibition of a microbiota-derived peptide ameliorates established acute lung injury. *Am J Pathol*. 2023;193:740–54.
- [30] Fujiwara K, Kobayashi T, Fujimoto H, Nakahara H, D'Alessandro-Gabazza CN, Hinneh JA, Takahashi Y, Yasuma T, Nishihama K, Toda M, Kajiki M, Takei Y, Taguchi O, Gabazza EC. Inhibition of cell apoptosis and amelioration of pulmonary fibrosis by thrombomodulin. *Am J Pathol*. 2017;187:2312–22.
- [31] Gabazza EC, Kasper M, Ohta K, Keane M, D'Alessandro-Gabazza C, Fujimoto H, Nishii Y, Nakahara H, Takagi T, Menon AG, Adachi Y, Suzuki K, Taguchi O. Decreased expression of aquaporin-5 in bleomycin-induced lung fibrosis in the mouse. *Pathol Int*. 2004;54:774–80.
- [32] Shimizu S, Gabazza EC, Taguchi O, Yasui H, Taguchi Y, Hayashi T, Ido M, Shimizu T, Nakagaki T, Kobayashi H, Fukudome K, Tsuneyoshi N, D'Alessandro-Gabazza CN, Izumizaki M, Iwase M, Homma I, Adachi Y, Suzuki K. Activated protein C inhibits the expression of platelet-derived growth factor in the lung. *Am J Respir Crit Care Med*. 2003;167:1416–26.
- [33] Antoniak S, Tatsumi K, Hisada Y, Milner JJ, Neidich SD, Shaver CM, Pawlinski R, Beck MA, Bastarache JA, Mackman N. Tissue factor deficiency increases alveolar hemorrhage and death in influenza A virus-infected mice. *J Thromb Haemost*. 2016;14:1238–48.
- [34] Tatsumi K, Antoniak S, Subramaniam S, Gondouin B, Neidich SD, Beck MA, Mickelson J, Monroe DM 3rd, Bastarache JA, Mackman N. Anticoagulation increases alveolar hemorrhage in mice infected with influenza A. *Physiol Rep*. 2016;4:e13071.
- [35] Shibamiya A, Hersemeyer K, Schmidt Woll T, Sedding D, Daniel JM, Bauer S, Koyama T, Preissner KT, Kanse SM. A key role for Toll-like receptor-3 in disrupting the hemostasis balance on endothelial cells. *Blood*. 2009;113:714–22.
- [36] Piton G, Capellier G. Biomarkers of gut barrier failure in the ICU. *Curr Opin Crit Care*. 2016;22:152–60.
- [37] FitzGerald ES, Chen Y, Fitzgerald KA, Jamieson AM. Lung epithelial cell transcriptional regulation as a factor in COVID-19-associated coagulopathies. *Am J Respir Cell Mol Biol*. 2021;64:687–97.
- [38] Mackman N, Grover SP, Antoniak S. Tissue factor expression, extracellular vesicles, and thrombosis after infection with the respiratory viruses influenza A virus and coronavirus. *J Thromb Haemost*. 2021;19:2652–8.
- [39] Sachetto ATA, Mackman N. Tissue factor and COVID-19: an update. *Curr Drug Targets*. 2022;23:1573–7.
- [40] Rotoli BM, Barilli A, Visigalli R, Ferrari F, Dall'Asta V. Endothelial cell activation by SARS-CoV-2 spike S1 protein: a crosstalk between endothelium and innate immune cells. *Biomedicines*. 2021;9:1220.
- [41] Bevers EM, Williamson PL. Getting to the outer leaflet: physiology of phosphatidylserine exposure at the plasma membrane. *Physiol Rev*. 2016;96:605–45.
- [42] Dahlback B. Natural anticoagulant discovery, the gift that keeps on giving: finding FV-Short. *J Thromb Haemost*. 2023;21:716–27.
- [43] Iba T, Levy JH, Levi M, Thachil J. Coagulopathy in COVID-19. *J Thromb Haemost*. 2020;18:2103–9.
- [44] Budhbraja A, Basu A, Gheware A, Abhilash D, Rajagopala S, Pakala S, Sumit M, Ray A, Subramaniam A, Mathur P, Nambirajan A, Kumar S, Gupta R, Wig N, Trikha A, Guleria R, Sarkar C, Gupta I, Jain D. Molecular signature of postmortem lung tissue from COVID-19 patients suggests distinct trajectories driving mortality. *Dis Model Mech*. 2022;15:dmm049572.
- [45] Zhou J, Yang X, Yang Y, Wei Y, Lu D, Xie Y, Liang H, Cui P, Ye L, Huang J. Human microbiota dysbiosis after SARS-CoV-2 infection have the potential to predict disease prognosis. *BMC Infect Dis*. 2023;23:841.
- [46] Nishiwaki R, Imoto I, Oka S, Yasuma T, Fujimoto H, D'Alessandro-Gabazza CN, Toda M, Kobayashi T, Osamu H, Fujibe K, Nishikawa K, Hamaguchi T, Sugimasa N, Noji M, Ito Y, Takeuchi K, Cann I, Inoue Y, Kato T, Gabazza EC. Elevated plasma and bile levels of corisin, a microbiota-derived proapoptotic peptide, in patients with severe acute cholangitis. *Gut Pathog*. 2023;15:59.
- [47] Fajgenbaum DC, June CH. Cytokine storm. *N Engl J Med*. 2020;383:2255–73.
- [48] Kaiser R, Leunig A, Pekayvaz K, Popp O, Joppich M, Polewka V, Escaig R, Anjum A, Hoffknecht ML, Gold C, Brambs S, Engel A, Stockhausen S, Knottenberg V, Titova A, Haji M, Scherer C, Muenchhoff M, Hellmuth JC, Saar K, et al. Self-sustaining IL-8 loops drive a prothrombotic neutrophil phenotype in severe COVID-19. *JCI Insight*. 2021;6:e150862.
- [49] Qin Z, Liu F, Blair R, Wang C, Yang H, Mudd J, Currey JM, Iwanaga N, He J, Mi R, Han K, Midkiff CC, Alam MA, Aktas BH, Heide RSV, Veazey R, Piedimonte G, Maness NJ, Ergun S, Mauvais-Jarvis F, et al. Endothelial cell infection and dysfunction, immune activation in severe COVID-19. *Theranostics*. 2021;11:8076–91.
- [50] Mackman N, Antoniak S, Wolberg AS, Kasthuri R, Key NS. Coagulation abnormalities and thrombosis in patients infected with SARS-CoV-2 and other pandemic viruses. *Arterioscler Thromb Vasc Biol*. 2020;40:2033–44.
- [51] Zhang F, Lau RI, Liu Q, Su Q, Chan FKL, Ng SC. Gut microbiota in COVID-19: key microbial changes, potential mechanisms and clinical applications. *Nat Rev Gastroenterol Hepatol*. 2022;1–15.
- [52] Merenstein C, Bushman FD, Collman RG. Alterations in the respiratory tract microbiome in COVID-19: current observations and potential significance. *Microbiome*. 2022;10:165.

#### SUPPLEMENTARY MATERIAL

The online version contains supplementary material available at <https://doi.org/10.1016/j.jtha.2024.02.014>.